

SKA Key science project: Radio observations of cosmic reionization and first light

C.L. Carilli^{*†}

National Radio Astronomy Observatory, Socorro, NM, USA

E-mail: ccarilli@nrao.edu

I update the SKA key science program (KSP) on first light and cosmic reionization. The KSP has two themes: (i) Using the 21cm line of neutral hydrogen as the most direct probe into the evolution of the neutral intergalactic medium during cosmic reionization. Such HI 21cm studies are potentially the most important new window on cosmology since the discovery of the CMB. (ii) Observing the gas, dust, star formation, and dynamics, of the first galaxies and AGN. Observations at cm and mm wavelengths, provide an unobscured view of galaxy formation within 1 Gyr of the Big Bang, and are an ideal complement to the study of stars, ionized gas, and AGN done using near-IR telescopes. I summarize HI 21cm signals, challenges, and telescopes under construction. I also discuss the prospects for studying the pre-galactic medium, prior to first light, using a low frequency telescope on the Moon. I then review the current status of mm and cm observations of the most known distant galaxies ($z \geq 6$). I make the simple argument that even a 10% SKA-high demonstrator will have a profound impact on the study of the first galaxies. In particular, extending the SKA to the 'natural' atmospheric limit (set by the O₂ line) of ~ 45 GHz, increases the effective sensitivity to thermal emission by another factor four.

From planets to dark energy: the modern radio universe

October 1-5 2007

University of Manchester, Manchester, UK

*Speaker.

†The National Radio Astronomy Observatory (NRAO) is operated by Associated Universities, Inc. under a cooperative agreement with the National Science Foundation.

1. Introduction

Cosmic reionization corresponds to the transition from a fully neutral intergalactic medium (IGM) to an (almost) fully ionized IGM caused by the UV radiation from the first luminous objects. Reionization is a key benchmark in cosmic structure formation, indicating the formation of the first luminous objects. Reionization, and the preceding 'dark ages', remain the last of the major phases of cosmic evolution left to explore.

The SKA international science advisory committee identified cosmic reionization and first light as one of the key science projects for a future square kilometer array. The KSP had two parts:

- Use the 21cm line of neutral hydrogen as the most direct probe into the evolution of the neutral intergalactic medium during cosmic reionization. Such HI 21cm studies are potentially the most important new window on cosmology since the discovery of the CMB.
- Observe the gas, dust, star formation, and dynamics, of the first galaxies and AGN. Observations at cm and mm wavelengths, provide an unobscured view of galaxy formation within 1 Gyr of the Big Bang, and are an ideal complement to the study of stars, ionized gas, and AGN done using near-IR telescopes.

I should start with a mea culpa: the original SKA KSP was misnamed as study of the 'dark ages'. The dark ages correspond to the period prior to reionization and first light, while the SKA KSP focuses on essentially cosmic reionization, which signals the end of the dark ages. This review will focus again on reionization, although I have included a summary of recent work suggesting that the dark ages themselves may be a gold mine of cosmological discoveries through the HI 21cm studies of the pre-galactic medium, potentially studied with a low frequency radio telescope on the Moon (section 3.5).

Since this KSP was first proposed (Carilli et al. 2004), there has been an explosion in theoretical studies of the expected HI 21cm signal from reionization, as well as extensive reviews written on the first galaxies and the process of reionization (Furlanetto, Oh, Briggs 2007; Ellis 2007; Fan, Carilli, Keating 2007). In this review, I will concentrate on updating predicted signals, observational challenges, and telescopes under construction. More on the theory of reionization can be found in Ferrara (this volume).

In Section 4, I present the latest results on studies of the most distant galaxies ($z \geq 6$), and a look toward the promise of a 10% SKA demonstrator working at short cm wavelengths for such studies. I begin with a brief review of the current observational constraints on cosmic reionization. For more detail, see Fan, Carilli, Keating (2006).

2. Observational constraints on cosmic reionization

The last decade has seen the first observational evidence for cosmic reionization. The primary results come from the Gunn-Peterson effect, ie. $\text{Ly}\alpha$ absorption by the neutral IGM, toward the most distant quasars ($z \sim 6$), and the large scale polarization of the CMB, corresponding to Thomson scattering during reionization. These observations suggest that reionization was a complex process, with significant variance in both space and time, starting perhaps as high as $z \sim 14$, with

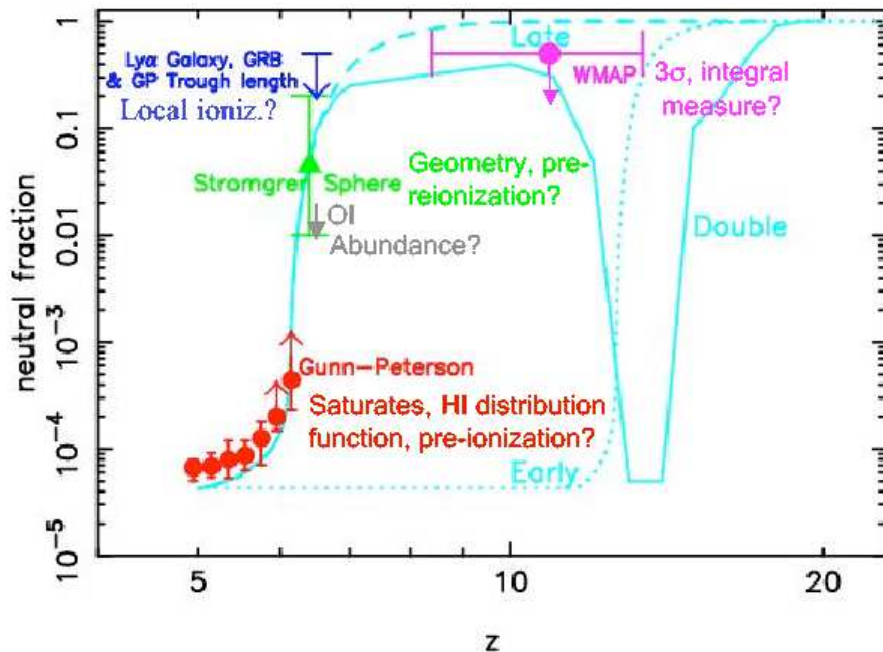


Figure 1: The neutral fraction, by volume, of the intergalactic medium as a function of redshift. Current constraints are shown, as well as representative models for the HI evolution. Also shown are potential causes for uncertainty in the measurements (adapted from Fan, Carilli, Keating 2006).

the last vestiges of the the neutral IGM being etched-away by $z \sim 6$ (see review by Fan, Carilli, Keating 2006).

Figure 1 shows the current state of observational constraints on the cosmic neutral fraction as a function of redshift. The GP effect, and related statistical measures of eg. dark gaps in QSO spectra (Fan et al. 2006), suggest a qualitative change in the nature of the IGM at $z \sim 6$, likely signifying the end of reionization. At the other extreme, the CMB large scale polarization suggests a significant ionization fraction extending to $z \sim 11$. A major task in the coming decade is to 'connect the dots' from $z \sim 6$ out to $z \sim 14$ in this figure.

These first measurements of cosmic reionization are truly a water-shed event. However, it has also become clear that these important first probes of cosmic reionization are fundamentally limited. Figure 1 also lists potential causes for uncertainty in the measurements (adapted from Fan, Carilli, Keating 2006). The CMB polarization remains only a 3σ result, and it represents an integral measure of the Thomson scattering optical depth back to recombination, and hence can be fit by many different reionization scenarios. For the Gunn-Peterson effect, the IGM becomes optically thick to $\text{Ly}\alpha$ absorption for a neutral fraction $> 10^{-3}$, and hence the diagnostic capabilities of this probe effectively saturate at low neutral fractions. The GP conclusions are also depend on an assumed clumping factor for the IGM.

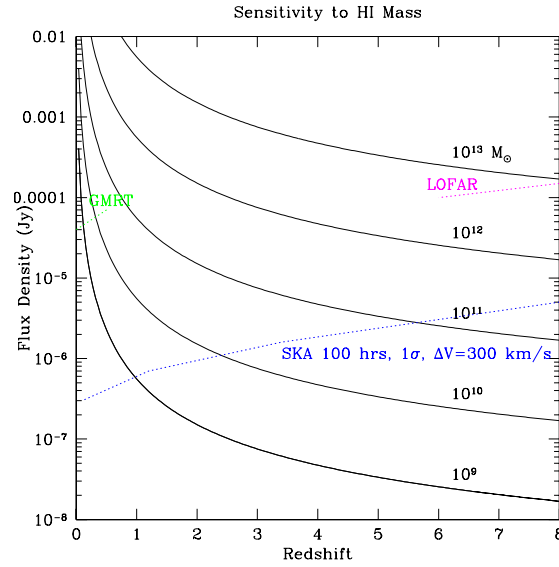


Figure 2: The predicted HI 21cm signals versus redshift for different HI masses, assuming a constant line width of 300 km s⁻¹. Sensitivity of low frequency telescopes are also shown, for 1000 hour integration with LOFAR and the GMRT, and 100 hour with SKA.

3. HI 21cm signals from cosmic reionization

3.1 Large Scale Structure

It is widely recognized that the most direct and incisive means of studying cosmic reionization is through the 21cm line of neutral Hydrogen (Furlanetto et al. 2006; Carilli 2006). The study of HI 21cm emission from cosmic reionization entails the study of large scale structure (LSS), meaning HI masses $> 10^{12} M_{\odot}$.

Figure 2 shows the signal strength expected for a given HI mass versus redshift. A constant line width of 300 km s⁻¹ was assumed for simplicity. The key point is that, even with future large area telescopes such as the SKA, HI measurements at these high redshifts will be restricted to LSS, not individual galaxies. Fortunately, during this epoch the entire IGM can be neutral, and the LSS in question is not simply mass clustering, but involves a combination of structure in cosmic density, neutral fraction, and HI excitation temperature.

The optical depth on the 21cm line of neutral hydrogen is given by:

$$\tau = \frac{3c^3 \hbar A_{10} n_{HI}}{16k_B v_{21}^2 T_S H(z)} \sim 0.0074 \frac{x_{HI}}{T_S} (1 + \delta) (1 + z)^{3/2} [H(z) / (\frac{dv}{dr})], \quad (3.1)$$

where A is the Einstein coefficient and $v_{21} = 1420.40575$ MHz (eg. Santos et al. 2005). This equation shows immediately the rich physics involved in studying the HI 21cm line during reionization, with τ depending on the evolution of cosmic over-densities, δ (predominantly in the linear regime), the neutral fraction, x_{HI} (ie. reionization), the HI excitation, or spin, temperature, T_S , and the velocity structure, $\frac{dv}{dr}$, including the Hubble flow and peculiar velocities.

In the Rayleigh-Jeans limit, the observed brightness temperature (relative to the CMB) due to the HI 21cm line at a frequency $\nu = \nu_{21}/(1+z)$, is given by:

$$T_B \approx \frac{T_S - T_{CMB}}{1+z} \tau \approx 7(1+\delta)_{XHI} \left(1 - \frac{T_{CMB}}{T_S}\right) (1+z)^{1/2} \text{ mK}, \quad (3.2)$$

The conversion factor from brightness temperature to specific intensity, I_ν , is given by: $I_\nu = \frac{2k_B}{(\lambda_{21}(1+z))^2} T_B = 22(1+z)^{-2} T_B \text{ Jy deg}^{-2}$. These equations show that for $T_S \sim T_{CMB}$ one expects no 21cm signal. When $T_S \gg T_{CMB}$, the brightness temperature becomes independent of spin temperature. When $T_S \ll T_{CMB}$, we expect a strong negative (ie. absorption) signal against the CMB.

The interplay between the CMB temperature, the kinetic temperature, and the spin temperature, coupled with radiative transfer, lead to a number of interesting physical regimes for the HI 21cm signal (Ali 2005; Barkana & Loeb 2004; Carilli 2005; Furlanetto et al. 2006; Fan, Carilli, Keating 2006):

- At $z > 200$ equilibrium between T_{CMB} , T_K , and T_S is maintained by Thomson scattering off residual free electrons and gas collisions. In this case $T_S = T_{CMB}$ and there is no 21cm signal.
- At $z \sim 30$ to 200, the gas cools adiabatically, with temperature falling as $(1+z)^2$, ie. faster than the $(1+z)$ for the CMB. However, the mean density is still high enough to couple T_S and T_K , and the HI 21cm signal would be seen in absorption against the CMB (Sethi 2005; see section 3.5).
- At $z \sim 20$ to 30, collisions can no longer couple T_K to T_S , and T_S again approaches T_{CMB} . However, the Ly α photons from the first luminous objects (Pop III stars or mini-quasars), may induce local coupling of T_K and T_S , thereby leading to some 21cm absorption regions (Cen 2006). At the same time, Xrays from these same objects could lead to local IGM warming above T_{CMB} (Chen & Miralda-Escude 2003). Hence one might expect a patch-work of regions with no signal, absorption, and perhaps emission, in the 21cm line.
- At $z \sim 6$ to 20 all the physical processes come to play. The IGM is being warmed by hard Xrays from the first galaxies and black holes (Loeb & Zaldarriaga 2004; Barkana & Loeb 2004; Ciardi & Madau 2003), as well as by weak shocks associated with structure formation (Furlanetto, Zaldarriaga, & Hernquist 2005), such that T_K is likely larger than T_{CMB} globally (Furlanetto et al. 2004b). Likewise, these objects are reionizing the universe, leading to a fundamental topological change in the IGM, from the linear evolution of large scale structure, to a bubble dominated era of HII regions (Furlanetto et al. 2005a).

3.2 The HI 21cm signals

Global signal: The left panel in Figure 3 shows predictions of the global (all sky) increase in the background temperature due to the HI 21cm line from the neutral IGM (Gnedin & Shaver 2003). The predicted HI signal peaks at roughly 20 mK above the foreground at $z \sim 10$. At higher redshift, prior to IGM warming, but allowing for Ly α emission from the first luminous objects, the HI is seen in absorption against the CMB. Since this is an all sky signal, the sensitivity of the experiment is independent of telescope collecting area, and the experiment can be done

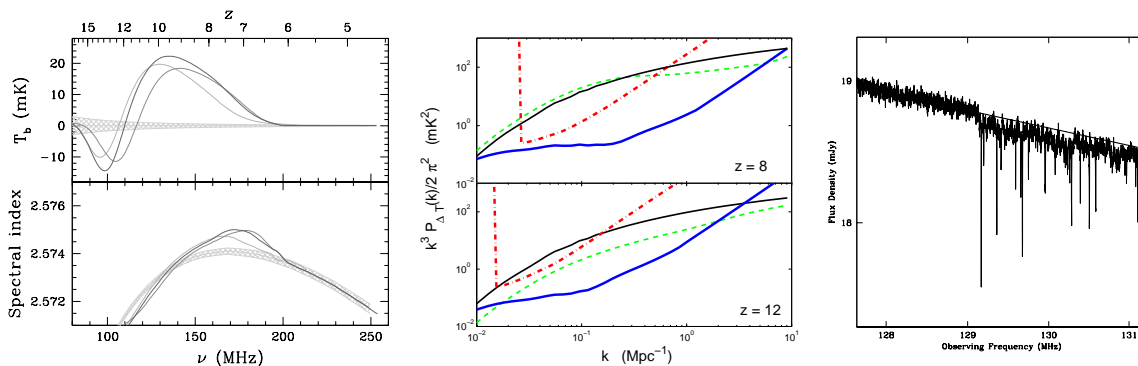


Figure 3: **Left:** Global (all sky) HI signal from reionization (Gnedin & Shaver 2003). The shaded region shows the expected thermal noise in a carefully controlled experiment. **Center:** Predicted HI 21cm brightness temperature power spectrum (in log bins) at redshifts 8 and 12 (McQuinn et al. 2006). The thin black line shows the signal when density fluctuations dominate. The dashed green line shows the predicted signal for $\bar{x}_i = 0.2$ at $z = 12$, and $\bar{x}_i = 0.6$ at $z = 8$, in the (Furlanetto et al. 2004) semi-analytic model. The thick blue line shows the SKA sensitivity in 1000hrs. The thick red dot-dash show the sensitivity of the pathfinder experiment LOFAR. The cutoff at low k is set by the primary beam. **Right:** The simulated SKA spectrum of a radio continuum source at $z = 10$ (Carilli et al. 2002). The straight line is the intrinsic power law (synchrotron) spectrum of the source. The noise curve shows the effect of the 21cm line in the neutral IGM, including noise expected for the SKA in a 100 hour integration.

using small area telescopes at low frequency, with very well controlled, and calibrated, frequency response (Bowman, Rogers, Hewitt 2007). Note that the line signal is only $\sim 10^{-4}$ that of the mean foreground continuum emission at ~ 150 MHz.

Power spectra: The middle panel in Figure 3 shows the predicted power spectrum of spatial fluctuations in the sky brightness temperature due to the HI 21cm line (McQuinn et al. 2006). For power spectral analyses the sensitivity is greatly enhanced relative to direct imaging due to the fact that the universe is isotropic, and hence one can average the measurements in annuli in the Fourier (uv) domain, ie. the statistics of fluctuations along an annulus in the uv -plane are equivalent. Moreover, unlike the CMB, HI line studies provide spatial and redshift information, and hence the power spectral analysis can be performed in three dimensions. The rms fluctuations at $z = 10$ peak at about 10 mK rms on scales $\ell \sim 5000$.

A recent analysis by Lidz et al. (2008) shows that the MWA should be able to determine the HI 21cm power-spectrum over roughly a decade in wavenumber, $k \sim 0.1$ to $1h \text{ Mpc}^{-1}$. These data should be able to constrain both the amplitude and slope of the power spectrum. A key aspect of these measurements is determination of the redshift evolution of these quantities, with the amplitude of the rms power in the HI 21cm fluctuations peaking at redshift when the IGM is roughly 50% neutral.

Absorption toward discrete radio sources: An interesting alternative to emission studies is the possibility of studying smaller scale structure in the neutral IGM by looking for HI 21cm absorption toward the first radio-loud objects (AGN, star forming galaxies, GRBs) (Carilli et al. 2002). The rightpanel of Figure 3 shows the predicted HI 21cm absorption signal toward a high

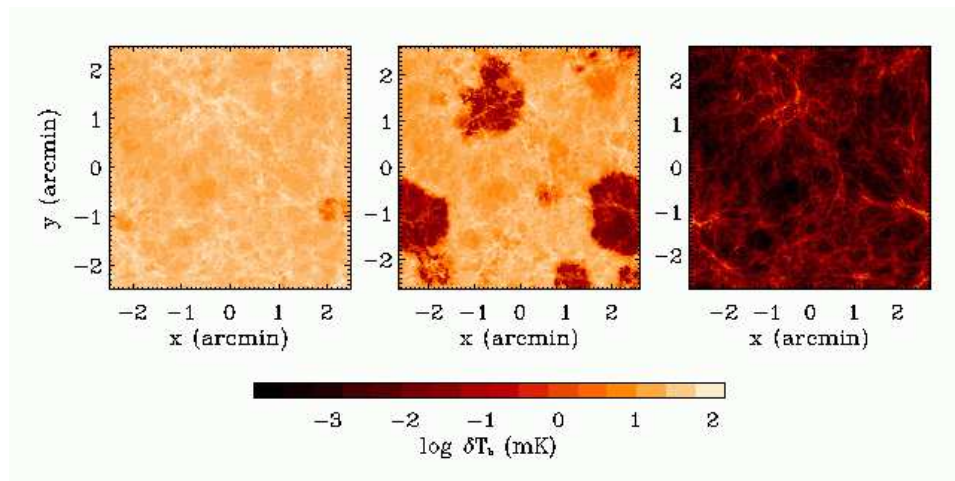


Figure 4: The simulated HI 21cm brightness temperature distribution during reionization at $z = 12, 9, 7$ (left to right) (Zaldariagga et al. 2004)

redshift radio source due to the ‘cosmic web’ prior to reionization, based on numerical simulations. For a source at $z = 10$, these simulations predict an average optical depth due to 21cm absorption of about 1%, corresponding to the ‘radio Gunn-Peterson effect’, and about five narrow (few km/s) absorption lines per MHz with optical depths of a few to 10%. These latter lines are equivalent to the Ly α forest seen after reionization (a recent treatment of this problem can be found in Furlanetto 2006). Furlanetto & Loeb (2002) predict a similar HI 21cm absorption line density due to gas in minihalos as that expected for the 21cm forest.

Tomography: Figure 4 shows the expected evolution of the HI 21cm signal during reionization based on numerical simulations (Zaldariagga et al. 2004; see also Zahn et al. 2007; Iliev et al. 2006; Shapiro et al. 2006, etc...). In this simulation, the HII regions caused by galaxy formation are seen in the redshift range $z \sim 8$ to 10, reaching scales up to $2'$ (frequency widths ~ 0.3 MHz ~ 0.5 Mpc physical size). These regions have (negative) brightness temperatures up to 20 mK relative to the mean HI signal. This corresponds to $5\mu\text{Jy beam}^{-1}$ in a $2'$ beam at 140 MHz. Only the full SKA will be able to image such structures.

Largest Cosmic Stromgren Spheres (CSS): While direct detection of the typical structure of HI and HII regions may be out of reach of the near-term EoR 21cm telescopes, there is a chance that even this first generation of telescopes will be able to detect the rare, very large scale HII regions associated with luminous quasars near the end of reionization. The expected signal is $\sim 20\text{mK} \times x_{HI}$ on a scale $\sim 10'$ to $15'$, with a line width of ~ 1 to 2 MHz (Wyithe, Loeb, Barnes 2005). This corresponds to $0.5 \times x_{HI}$ mJy beam^{-1} , for a $15'$ beam at $z \sim 6$ to 7, where x_{HI} is the IGM neutral fraction. Figure 5 shows a simulation of the expected images from near-term reionization telescopes, such as the MWA, for these very large structures. The key aspect of these systems is that the structures are three dimensional, making them much easier to detect than continuum structures at a similar brightness.

Wyithe et al. (2005) predict that, for late reionization, there should be several tens of (mostly fossil) large ($> 4\text{Mpc}$ physical) CSS per 10° field of view in $z \sim 6$ to 8. An interesting addition to the QSO CSS studies is the possibility that massive galaxy formation at very high redshift is highly

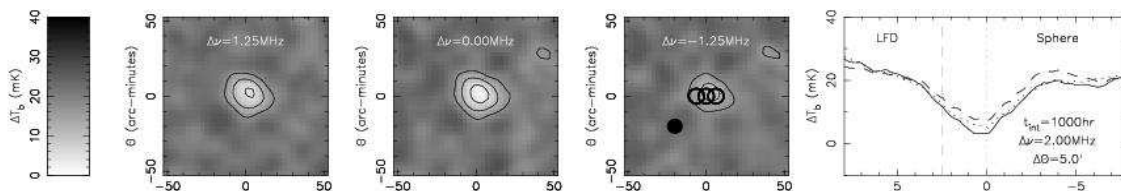


Figure 5: The simulated HI 21cm brightness temperature distribution for the largest expected structures during reionization, those associated with luminous QSOs, or highly clustered massive galaxy formation (Wyithe, Loeb, Barnes 2005). Left shows channel images with 1.25 MHz width, and right shows the spectrum at the position of the source.

clustered, occurring in rare peaks in the cosmic density field. The total number of ionizing photons from star formation integrated over the lifetime of the system can match that radiated by a luminous QSO (Li et al. 2007; Wyithe et al. 2007), and hence generate CSS comparable to those predicted for the QSOs. The star forming systems will both increase the size of the spheres around bright QSOs (since QSO and massive galaxy formation are likely to be coupled), as well as increase the number of large spheres, in cases where the QSO has not turned-on yet.

To add a personal bias to this review, my prediction is that the first robust detection of the neutral IGM using the 21cm line will not be through power-spectral studies, but come through a repeatable, very large, three dimensional 'hole' seen in images made in the very wide, deep field ($\Delta\theta \geq 10^\circ$, $\Delta z \geq 2$), with up-coming reionization telescopes.

3.3 Telescopes

Table 1 summarizes the current experiments under construction to study the HI 21cm signal from cosmic reionization. These experiments vary from single dipole antennas to study the all-sky signal, to 10,000 dipole arrays to perform the power spectral analysis, and potentially to image the largest structures during reionization (eg. the quasar Stromgren spheres).

Most of the experiments have a few to 10% of the collecting area of the SKA, and there are many common features:

- All rely on some form of a wide-band dipole or spiral antenna, eg. log-periodic yagis, sleeve dipoles, or bow-ties, with steering of the array response through electronic phasing of the elements.
- The front-end electronics are relatively simple (uncooled amplifier/balun), since the system performance is dominated by the sky brightness temperature.
- Most rely on a grouping of dipoles into 'tiles' or 'stations', to decrease the field-of-view, and to decrease the data rate into the correlator to a manageable level.
- The large number of array elements, and the need for wide-field, high dynamic range imaging over an octave, or more, of bandwidth, demand major computing resources, both for basic cross-correlation, and subsequent calibration, imaging, and analysis. For example, assuming an array of 1000 tiles, a 100 MHz bandwidth, and 8 bit sampling, the total data rate coming into the correlator is 1.6 Tbit s^{-1} . The LOFAR array is working with IBM to apply the 27.4 Tflop Blue Gene supercomputing technology to interferometric imaging (Falcke 2006).

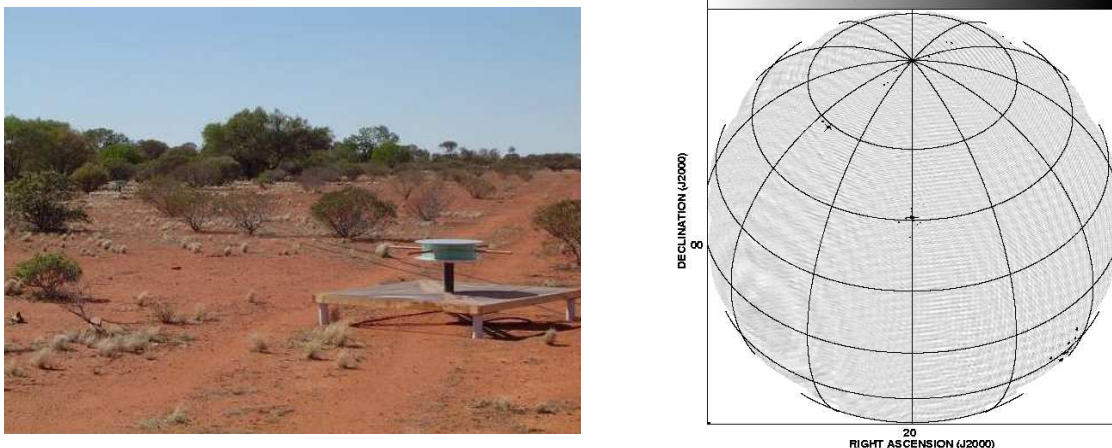


Figure 6: Left: A few elements of the PAPER test array in Western Australia (Mastrantonio & Backer 2007 in prep). Right: A full sky image from PAPER-GB showing the brightest sources (Cas A, Cygnus A, Sun).

First results from these path-finder telescopes are expected within the next few years. Experience from these observations in dealing with the interference, ionosphere, and wide-field imaging/dynamic range problems will provide critical information for future experiments, such as the Square Kilometer Array, or a low frequency radio telescope on the moon.

As an example, Figure 6 shows dipole elements and an all sky image from the Precision Array to Probe the Epoch of Reionization (PAPER). This array is being built in Western Australia, with a test installation in Green Bank, with the purpose of performing near-term studies of the HI 21cm signal from reionization.

3.4 Observational challenges to HI 21cm studies of cosmic reionization

Foregrounds: The HI 21cm signal from reionization must be detected on top of a much larger synchrotron signal from foreground emission. This foreground includes discrete radio galaxies, and large scale emission from our own Galaxy. The expected HI 21cm signal is about 10^{-4} of the foreground emission at 140 MHz.

di Matteo et al. (2002) show that, even if point sources can be removed to the level of $1 \mu\text{Jy}$, the rms fluctuations on spatial scales $\leq 10'$ ($\ell \geq 1000$) due to residual radio point sources will be $\geq 10 \text{ mK}$ just due to Poisson noise, increasing by a factor 100 if the sources are strongly clustered (see also di Matteo, Ciardi, & Miniati 2004; Oh & Mack 2003).

A key point is that the foreground emission should be smooth in frequency, predominantly the sum of power-law, or perhaps gently curving, non-thermal spectra. A number of complimentary approaches have been presented for foreground removal (Morales, Bowman, & Hewitt 2005). Gnedin & Shaver (2003) and Wang et al (2005) consider fitting smooth spectral models (power laws or low order polynomials in log space) to the observed visibilities or images. Morales & Hewitt (2003) and Morales (2004) present a 3D Fourier analysis of the measured visibilities, where the third dimension is frequency. The different symmetries in this 3D space for the signal arising from the noise-like HI emission, versus the smooth (in frequency) foreground emission, can be a powerful means of differentiating between foreground emission and the EoR line signal. Santos et

Experiment	Site	Type	ν range MHz	Area m ²	Date	Goal
Mark I ^a	Australia	spiral	100-200	few	2007	All Sky
EDGES ^b	Australia	four-point	100-200	few	2007	All Sky
GMRT ^c	India	parabola array	150-165	4e4	2007	CSS ^d
PAPER ^e	Australia	dipole array	110-190	1e3	2008	PS/CSS/Abs
21CMA ^f	China	dipole array	70-200	1e4	2007	PS
MWAd ^g	Australia	aperture array	80-300	1e4	2008	PS/CSS/Abs
LOFAR ^h	Netherlands	aperture array	115-240	1e5	2008	PS/CSS/Abs
SKA ⁱ	?	aperture array	100-200	1e6	2015	Imaging

Table 1: HI 21cm Cosmic Reionization Experiments

^ahttp://www.atnf.csiro.au/news/newsletter/jun05/Cosmological_re-ionization.htm

^b<http://www.haystack.mit.edu/ast/arrays/Edges/index.html>

^c<http://gmrt.ncra.tifr.res.in/>

^dCSS = Cosmic Stromgren Spheres, PS = power spectrum, Abs = absorption

^e<http://astro.berkeley.edu/~dbacker/EoR/>

^f<http://cosmo.bao.ac.cn/project.html>

^g<http://www.haystack.mit.edu/ast/arrays/mwa/>

^h<http://www.lofar.org/>

ⁱ<http://www.skatelescope.org/>

al. (2005), Bharadwaj & Ali (2005), Zaldariagga et al. (2004a) perform a similar analysis, only in the complementary Fourier space, meaning cross correlation of spectral channels. They show that the 21cm signal will effectively decorrelate for channel separations > 1 MHz, while the foregrounds do not. The overall conclusion of these methods is that spectral decomposition should be adequate to separate synchrotron foregrounds from the HI 21cm signal from reionization at the mK level.

Glesser, Nusser, & Bensor (2008) recently considered the relative contribution of various contributions to the mean sky brightness temperature at low frequency. They show that roughly 90% comes from the Galactic synchrotron emission, close to 10% from extragalactic radio sources, and up to $\sim 2\%$ from Galactic free-free emission. They also show that these foregrounds can be removed effectively through image reconstruction techniques that take into consideration the very different frequency structure of the cosmological line signal and the foreground continuum emission.

Ionosphere: A second potential challenge to low frequency imaging over wide fields is phase fluctuations caused by the ionosphere. These fluctuations are due to index of refraction fluctuations in the ionized plasma, and behave as $\Delta\phi \propto \nu^{-2}$.

Figure 7 shows an example of ionospheric phase errors on source positions using VLA data at 74 MHz (Cotton et al. 2004; Lane et al. 2004). Positions of five sources are shown for a series of snap shot images over 10 hours. A number of interesting phenomena can be seen. First,

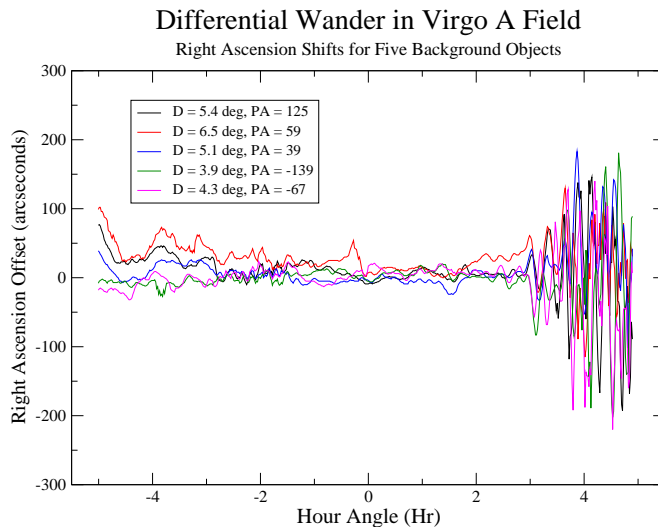


Figure 7: The positions of five sources in the Virgo A field at 74 MHz observed with the VLA over 10 hours (Cotton et al. 2004; Lane et al. 2004). The source positions vary with time due to fluctuations in the electronic path-length through the ionosphere.

the sources are slowly moving in position over time, by $\pm 50''$ over timescales of hours. These position shifts reflect the changing electronic path-length due to the fluctuating ionosphere (ie. tilts in the incoming wavefront due to propagation delay). Second, the individual sources move roughly independently. This is a demonstration of the 'isoplanatic patch' problem, ie. the excess electrical path-length is different in different directions. At 74 MHz, the typical coherent patch size is about 3° to 4° . Celestial calibrators further than this distance from a target source no longer give a valid solution for the combined instrumental and propagation delay term required to image the target source. And third, at the end of the observation there occurs an ionospheric storm, or traveling ionospheric disturbance, which effectively precludes coherent imaging during the event.

New wide field self-calibration techniques, involving multiple phase solutions over the field, or a 'rubber screen' phase model (Cotton et al. 2004), are being developed that should allow for self-calibration over wide fields.

Interference: Perhaps the most difficult problem facing low frequency radio astronomy is terrestrial (man-made) interference (RFI). The relevant frequency range corresponds to 7 to 200 MHz ($z = 200$ to 6). These are not protected frequency bands, and commercial allocations include everything from broadcast radio and television, to fixed and mobile communications.

Many groups are pursuing methods for RFI mitigation and excision (see Ellingson 2004). These include: (i) using a reference horn, or one beam of a phased array, for constant monitoring of known, strong, RFI signals, (ii) conversely, arranging interferometric phases to produce a null at the position of the RFI source, and (iii) real-time RFI excision using advanced filtering techniques in time and frequency, of digitized signals both pre- and post-correlation. The latter requires very high dynamic range (many bit sampling), and very high frequency and time resolution.

In the end, the most effective means of reducing interference is to go to the remotest sites.

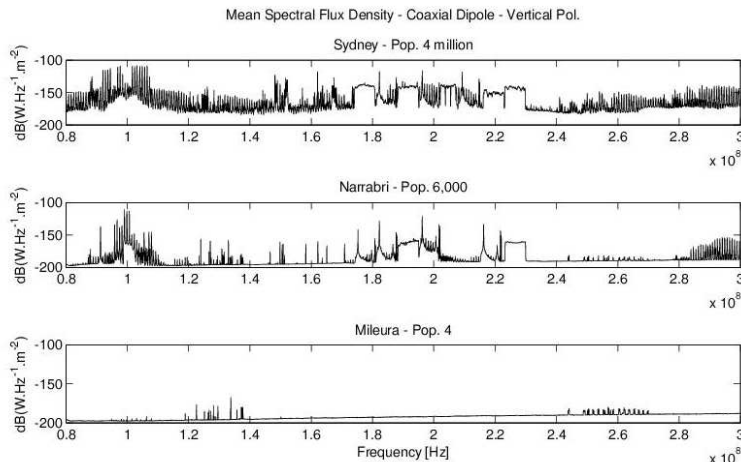


Figure 8: The interference environment in Australia. The FM band is between 87.5 and 108 MHz. The TV stations are between 180 and 200MHz, including broad band digital transmissions. Shown courtesy of A. Chippendale and R. Beresford (taken as part of the ATNF SKA Site Monitoring Program.)

Figure 8 shows the interference measured at three different locations with population densities changing by roughly four orders of magnitude (Chippendale & Beresford 2006 ATNF RFI monitoring program). The MWA, PAPER, and PAST have selected sites in remote regions of Western Australia, and China, because of known low RFI environments. Of course, the ultimate location would be the far-side of the moon (section 3.5).

The technical challenges to HI 21cm observations of reionization are many. Use of spectral decomposition to remove the foregrounds requires careful control of the synthesized beam as a function of frequency, with the optimal solution being a telescope design where the synthesized beam is invariant as a function of frequency (Bowman et al. 2007). High dynamic range front ends are required to avoid saturation in cases of strong interference, while fine spectral sampling is required to avoid Gibbs ringing in the spectral response. The polarization response must be stable and well calibrated to remove polarized foregrounds (Haverkorn et al. 2004). Calibration in the presence of a structured ionospheric phase screen requires new wide field calibration techniques. The very high data rate expected for many element ($\geq 10^3$) arrays requires new methods for data transmission, cross correlation, and storage.

3.5 The lunatic fringe: A PAPER Moon

At the lowest frequencies, ≤ 50 MHz or so, where we hope to study the Pre-galactic medium (PGM), phase fluctuations and the opacity of the ionosphere become problematic. There is long standing interest in building a low frequency radio telescope on the far side of the moon (Gorogolewski 1965; Burke 1985; Kuiper et al. 1990; Burns & Asbell 1991; Woan et al. 1997). The reasons are clear (section 2): no ionosphere, and shielding from terrestrial radio frequency interference (RFI). Two factors have acted to rekindle interest in low frequency radio astronomy from

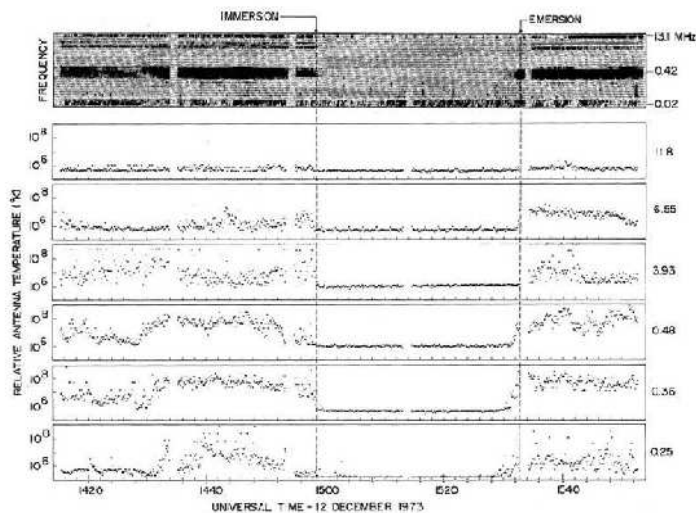


Figure 9: Radio power received by the lunar orbiting radio astronomy explorer satellite in 1973 (RAE2; Alexander et al. 1975). The power is dominated by the Earth’s auroral emission except during immersion, when the Earth is totally blocked by the moon.

moon. First, scientifically, efforts to study the PGM using the redshifted HI 21cm line have spurred numerous ground-based low frequency projects (section 3). And second is the new NASA initiative to return Man to the moon, and beyond.

While not a scientific rationale, it should be pointed out that a low frequency telescope may be the easiest astronomical facility to deploy and maintain on the moon. The antennas and electronics are high tolerance, with wavelengths $> 1.5\text{m}$ and system noise characteristics dominated by the Galactic foreground radiation. Deployment could be automated, using either javelin deployment (EADS/ASTRON), rollout of thin polyimide films with metallic deposits (ROLSS; Lazio et al. 2006), inflatable dipoles, or deployment by rovers. Likewise, being a phased array, low frequency telescopes are electronically steered, and hence have no moving parts. Lastly, there is no potential difficulty with lunar dust affecting the optics.

Figure 9 shows radio power received by a low frequency radio receiver on a lunar orbiter from the 1970’s (Alexander et al. 1975). The strong power received from Earth’s auroral emission is completely gone during immersion.

At the very low frequencies corresponding to the dark ages, going to the Moon becomes imperative, due to the rapidly increasing ionospheric opacity and phase effects. A number of studies have considered this very low frequency, pre-reionization HI 21cm signal (Loeb & Zaldarriaga 2004; Cen 2006; Barkana & Loeb 2005b; Shethi 2005). The HI 21cm measurements can explore this physical regime at $z \sim 50$ to 300, or redshifts $z > 30$.

In this redshift regime the HI generally follows linear density fluctuations, and hence the experiments are as clean as CMB studies, and $T_K < T_{CMB}$, so a relatively strong absorption signal might be expected. Also, Silk damping, or photon diffusion, erases structures on scales $\ell > 2000$ in the CMB at recombination, corresponding to comoving scales = 22 Mpc, leaving the 21cm studies

as the only current method capable of probing to very large ℓ in the linear regime. The predicted rms brightness temperature fluctuations are 1 to 10 mK on scales $\ell = 10^3$ to 10^6 ($0.2''$ to $1''$). These observations could provide the best test of non-Gaussianity of density fluctuations, and constrain the running power law index of mass fluctuations to large ℓ , providing important tests of inflationary structure formation. Sethi (2005) also suggests that a large global signal, up to -0.05 K, might be expected for this redshift range.

The difficulty in this case is one of sensitivity. The sky temperature is $> 10^4$ K, and using the equations in section 3.1, it is easy to show that, even if structures as bright at 10mK on scales of a few arcminutes exist, it would require ~ 10 square kilometers of collecting area to detect them. For the more typical small scale structure being considered (ie. $\sim 10''$), the required collecting area increases to 3.6×10^{10} m². The dynamic range requirements also become extreme, $> 10^8$. It should also be kept in mind that the sky becomes highly scattered due to propagation through interstellar and interplanetary plasma, with source sizes obeying: $\theta_{\min} \sim 1(\frac{v}{1\text{MHz}})^{-2}$ deg. Hence, all objects in the sky are smeared to $> 4''$ for frequencies < 30 MHz.

3.6 The HI n=2 fine structure line: An another probe of the neutral IGM?

Recently, Sethi et al. (2007) have proposed alternative study of the HI $2s_{1/2} - 2p_{3/2}$ transition (*in absorption*), with 9911 MHz rest frequency.¹ This transition has been notoriously difficult to detect in the nearby universe for two principal reasons related to the (large) Ly α Einstein A coefficient, $\sim 10^8$ s⁻¹ (Dennison et al. 2005). First, only $\sim 10^{-18}$ of atoms will be in the excited $2p$ state, since the lifetime is only a few nanoseconds; emission of a radio photon and decay to the $2s$ state is improbable. Second, the uncertainty principle dictates a ~ 100 MHz line width, due to the characteristic time scale for decay. Detecting such weak, broad lines is difficult. Additional factors relevant to the nearby universe include local dust absorption of Ly α photons that would otherwise pump the $2p$ state and collisional coupling of $2s$ and $2p$ in dense regions.

Sethi et al. argue that the situation for the pristine neutral IGM at high redshift may be different. Gunn-Peterson absorption toward quasars at $z > 6$ suggests that they are surrounded by ‘‘Cosmological Strömgren Spheres’’ (CSS), on physical scales of ~ 5 Mpc or $\sim 15'$ (Fan et al. 2006). The IGM outside the CSS could still be substantially neutral and relatively unperturbed. Non-ionizing UV photons between Ly α and the Lyman limit would propagate into the neutral medium, be absorbed, and be re-emitted as line radiation (e.g., resonant scattering of Ly α ; degradation of Ly β into H α ; two-photon decay $2s - 1s$). Sethi et al. show that through line scattering processes a tiny population in the metastable $2s$ state ($A \sim 8$ s⁻¹) can be maintained $\sim 10^8$ times longer than without the photon field excited by the quasar. Unlike the 21-cm transition, the fine structure transition would be seen in *absorption* against the microwave background.

Sethi et al. perform a detailed calculation of the expected brightness of the $2s_{1/2} - 2p_{3/2}$ transition. For an assumed UV radiation field and physical conditions in the IGM just outside a CSS around a $z \sim 6$ quasar, they predict a brightness temperature of $T_B \sim -20f_{\text{HI}} \mu\text{K}$. The prospect of 9911 MHz emission is promising for late reionization because it would be redshifted into the 1.4 GHz band, where existing dish antennas, and optimized feed and receiver systems, are available. In

¹Transitions among hyperfine components are at 9852, 9876, and 10030 MHz in a ratio of 1:5:2; Ershov 1987.

contrast, study of the redshifted HI 21cm line requires new facilities, VHF operation, and low-gain dipole feeds. Most importantly, the foregrounds are dramatically reduced at higher frequency.

There are some significant uncertainties in these calculations. The Ly α rate of 10^{58} s^{-1} assumed by Sethi et al. is $\sim 10\times$ higher than has been commonly estimated for high redshift quasars (e.g., Wyithe, Loeb, & Carilli 2005; Fan et al. 2006). However, re-estimation of statistical weights and consideration of other Lyman series transitions (Ly γ and above) balances revision in luminosity. Additional uncertainty surrounds the possibility of UV-absorbing dust in the early IGM due to early stellar processing and expulsion.

A straight-forward calculation shows that existing instruments such as the GBT, Parkes, and the most compact configuration of the ATNF, could potentially detect, or set interesting limits on, the neutral fraction of the IGM at $z \sim 6$ in reasonable integration times ~ 100 hours. The primary challenge in detecting $2s_{1/2} - 2p_{3/2}$ absorption will be achieving the very high spectral dynamic range required, of order 10^6 .

4. Radio studies of the first galaxies

4.1 Introduction

The last few years has seen remarkable advances in the discovery of luminous objects into cosmic reionization, ie. $z \geq 6$. This includes over 100 star forming galaxies discovered through the Ly-break and Ly α , and related, techniques (Ellis 2006), and some tens of QSOs (Fan et al. 2006). An important point to keep in mind when observing the first galaxies is that the GP effect precludes detection of these sources at observing wavelengths $\leq 900\text{nm}$. Hence, study of the first luminous objects is the regime of near-IR through radio astronomy, and hard X-rays.

Radio astronomy has also detected objects at $z \sim 6$ at cm and mm wavelengths in line and continuum emission. In this section I want to emphasize complementarity. Proper study of the complex process of galaxy formation requires observations across the electromagnetic spectrum. Near-IR observations reveal the ionized gas, stars, and AGN. Far IR through (sub)mm observations reveal the dust, higher order molecular line emission, and low excitation fine structure line emission. The higher cm frequencies reveal the lower order molecular transitions, which provide the best estimates of total gas mass. And at longer cm wavelengths one observes synchrotron emission, which is a dust-unbiased measure of the star formation rate and distribution, and of obscured AGN. The mm and cm studies are crucial to study the cool thermal material, the fuel for galaxy formation, and to probe galaxies in their earliest, dust-enshrouded stages of formation.

In this section I also emphasize the fact that a full SKA is not absolutely required for this program, and that a 10% Phase I SKA operating up to ~ 40 GHz would be a major step toward meeting this KSP (Carilli 2006).

4.2 The case of 1148+5251 at $z = 6.42$

To illustrate the power of our radio studies, we describe in some detail the particularly enlightening example of the most distant SDSS quasar, J1148+5251 at $z = 6.419$, a luminous broad line AGN with a black hole mass $\sim 10^9 M_{\odot}$ (Fan et al. 2004). The host galaxy has been detected in thermal dust, and non-thermal radio continuum, as well as molecular line emission, including

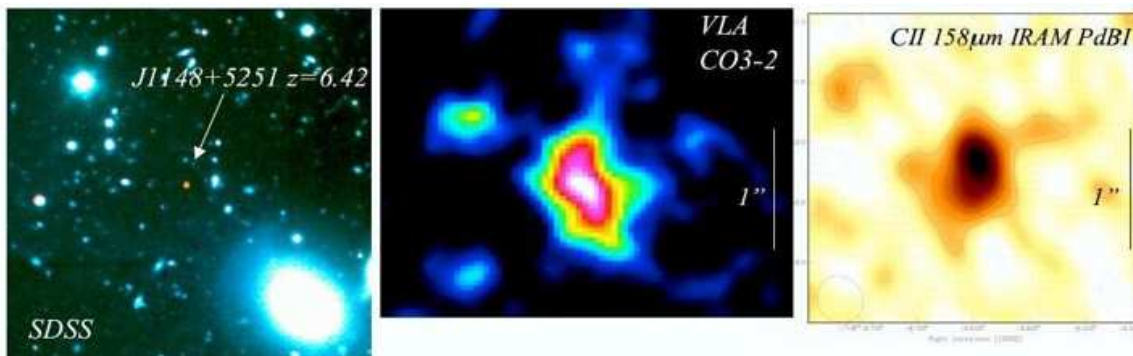


Figure 10: Images of the most distant SDSS QSO J1148+5251 at $z=6.42$. Left: The optical/nearIR SDSS color image (Fan et al. 2004). Center: The CO 3-2 emission from the host galaxy observed with NRAO's Very Large Array (Walter et al. 2004). Right: The CII 158 μ m emission observed with IRAM's Plateau de Bure Interferometer (Walter et al. in prep.). This supermassive black hole (black hole mass $\sim 10^9$ solar masses) is enveloped in a giant molecular gas cloud, with a molecular gas mass $\sim 2 \times 10^{10}$ solar masses, distributed over a physical scale of about 5.5kpc. The extended CII emission suggests active star formation across this region, with a total star formation rate ~ 3000 solar masses per year (Maiolino et al. 2006).

multiple CO transitions, and interesting limits to dense molecular gas tracers, such as HCN (Walter et al. 2003; Bertoldi et al. 2003; Carilli et al. 2004; Riechers et al. 2007).

Most recently, we have detected [CII] fine structure line emission from J1148+5251 (Maiolino et al. 2005). Fine structure lines are the dominant cooling mechanism for interstellar gas, and hence a key diagnostic of the energetics of the interstellar medium. Figure 10 shows the high resolution image of the [CII] and CO emission from J1148+5251. The [CII] and CO emission are co-spatial, and extended over a scale ~ 5.5 kpc, suggesting distributed gas heating, and hence star formation, on kpc-scales.

Figure 11 shows the rest-frame radio through near-IR SED of J1148+5251 (Wang et al. 2007). The source shows a clear excess in the FIR over the expected SED of a typical low z , optically selected QSO. This SED from the FIR through the radio is consistent with that expected for an active star forming galaxy with a dust temperature of ~ 50 K, and follows the radio-FIR correlation for star forming galaxies. Figure 4 also shows the CO excitation. The gas excitation is reasonably fit by an LVG model implying dense ($> 10^4 \text{ cm}^{-3}$), warm (≥ 50 K) molecular gas, comparable to what is seen in the centers of nearby nuclear starburst galaxies (Bertoldi et al. 2004).

These observations of J1148+5251, and other $z \sim 6$ QSOs (Carilli et al. 2007; Wang et al. 2007), demonstrate that large reservoirs of dust and metal enriched atomic and molecular gas can exist in massive galaxies within 1 Gyr of the Big Bang. The current observations suggest active star formation in the quasar host galaxy, with a massive star formation rate of order $10^3 M_{\odot} \text{ year}^{-1}$, adequate to form a large elliptical galaxy in a dynamical timescale $\sim 10^8$ years.

These observations of the host galaxies of the most distant quasars have inspired a number of major theoretical efforts aimed at delineating the formation of massive galaxies and supermassive blacks at the earliest epochs. In particular, the theory groups at Harvard and Arizona have performed state-of-the-art numerical simulations which follow the formation of the largest galaxies in the early Universe. In a series of recent papers (eg. Li et al. 2007; Narayanan et al. 2007),

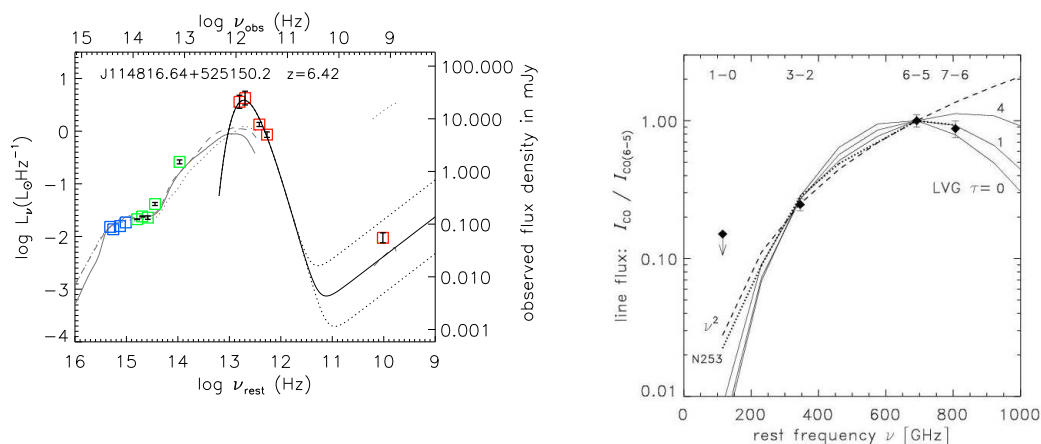


Figure 11: Left: The radio through near-IR SED of J1148+5251 (Wang et al. 2007). Right: The CO excitation in J1148+5251 (Bertoldi et al. 2003).

they show that early massive galaxy and SMBH formation is possible in rare peaks in the cosmic density field, through a series of gas-rich, massive mergers starting at $z \sim 14$. These systems evolve into massive galaxies at the centers of the most massive cluster environments seen today ($\sim 10^{15} M_{\odot}$). These results are generally consistent with the idea of 'downsizing' in both galaxy and supermassive black hole formation (Cowie et al. 1996; Heckman et al. 2004), meaning that the most massive black holes ($> 10^9 M_{\odot}$) and galaxies ($> 10^{12} M_{\odot}$) may form at high redshift in extreme, gas rich mergers/accretion events, in rare peaks in the cosmic density field.

4.3 The Coming Revolution: ALMA and a Phase I SKA

While radio astronomy has pushed back into cosmic reionization through these molecular line and continuum observations, current studies are at the limit of the capabilities of existing millimeter and radio telescopes. Even at these limits, these experiments stretch current instrumentation to the extreme limit, such that only rare and pathologic objects are detectable, ie. ultra- to hyper-luminous IR galaxies, with star formation rates $\geq 100 M_{\odot} \text{ year}^{-1}$. Fortunately, in the coming few years there will be dramatic improvements in observational capabilities at submillimeter through centimeter wavelengths that should revolutionize studies of the earliest galaxies.

An order of magnitude, or more, increase in collecting area at mm and cm wavelengths is required to enable the study of the first 'normal' galaxies within the epoch of reionization (EoR), eg. the $z \geq 6$ Ly α galaxies currently being discovered in deep near-IR surveys (SFRs ~ 10 to $100 M_{\odot} \text{ year}^{-1}$; eg. Murayama et al. 2007). At mm wavelengths this increase in capability will be realized when the Atacama Large Millimeter Array becomes operational early in the next decade. ALMA represents close to two orders of magnitude improvement in all areas of submillimeter astronomy, including: spatial resolution, spectral capabilities, and sensitivity. At cm wavelengths, the Expanded Very Large Array opens up the full frequency range from 1 to 50 GHz with order of magnitude improved continuum sensitivity, and dramatically improved spectral search capabilities. Unfortunately, the EVLA will still have the same total collecting area as the VLA. An increase in collecting area by roughly an order of magnitude over the EVLA is required at cm wavelengths to

match advances at other wavelength ranges, and perform the key, complementary science afford at the short cm wavelengths.

The key areas of science explored by these new facilities includes:

- *Dust and molecular gas:* ALMA, and a Phase I SKA (10% demonstrator $\sim 10\times$ EVLA collecting area) will reveal the dust and molecular gas in samples of normal star forming galaxies at $z > 6$, including *Lyalpha* emitters and Ly-break galaxies. These observations constrain the timescale for metal and dust enrichment in the most distant galaxies, and probe a key element in galaxy formation, namely the fundamental fuel for star formation.
- *Interstellar medium physics:* The physical conditions in the ISM of these galaxies (density, temperature, abundances) can be studied in detail, including gas excitation conditions, dust spectral energy distributions, and observations of dense gas tracers such as HCN and HCO+, directly associated with star forming regions.
- *Fine structure lines:* The [CII] 158 μ m line, and other atomic fine structure lines, are the dominant ISM gas cooling fine structure lines. These lines have great promise for exploring star formation, ISM physics, and galaxy dynamics, in the first normal galaxies. I expect these lines to be the 'work-horse' lines for studies of the first normal galaxies using ALMA.
- *Galaxy dynamics:* High resolution imaging of the distribution of molecular and ionized gas is the most direct method to determine the gas dynamics and dark matter content of the earliest galaxies. These observations also present the only method with which to test the M- σ relation for galaxies and black holes out to the highest redshifts.
- *Star formation:* The centimeter continuum emission associated with star formation in these galaxies can be observed, including millarcsecond resolution imaging using Very Long Baseline Interferometry.

4.4 Continuum examples

I illustrate the continuum studies with two recent examples. First, Figure 12 shows the results of a median stacking analysis of a sample of 6500 $z \sim 3$ LBGs in the COSMOS field. We obtain a robust statistical detection at 1.4 GHz of $0.9 \pm 0.15 \mu\text{Jy}$. Through the stacking analysis we are reaching sub- μJy sensitivity, ie. SKA-like depths, on galaxy populations at high redshift. The interesting implication is that the median star formation rate derived from the radio equals that derived from the median rest-frame UV emission, assuming the standard factor five dust correction for the UV emission. In other words, these data provide a critical, independent check on the standard reddening factor for high z LBGs (Carilli et al. in prep). We have also identified the first $z > 4$ submm galaxy, or massive dusty starburst, in these LBG samples (Capak et al. in prep).

Second, Figure 12 also shows a VLBA image with 28 μJy sensitivity of the most distant radio loud AGN, the $z = 6.12$ QSO J1427+3312 (McGreer et al. 2008; Momjian et al. 2008, in prep). The source has a steep spectral index of $\alpha_{1.4}^8 = -1.1$. The source is comprised of two dominant components separated by $\sim 170\text{pc}$, with a flux density ratio of about 4/1. Both components are clearly resolved by these observations, with sizes $\sim 60\text{pc}$. These data are consistent with J1427+3312 being a Compact Symmetric Object. CSOs are thought to be very young radio sources, $\leq 10^5$ years,

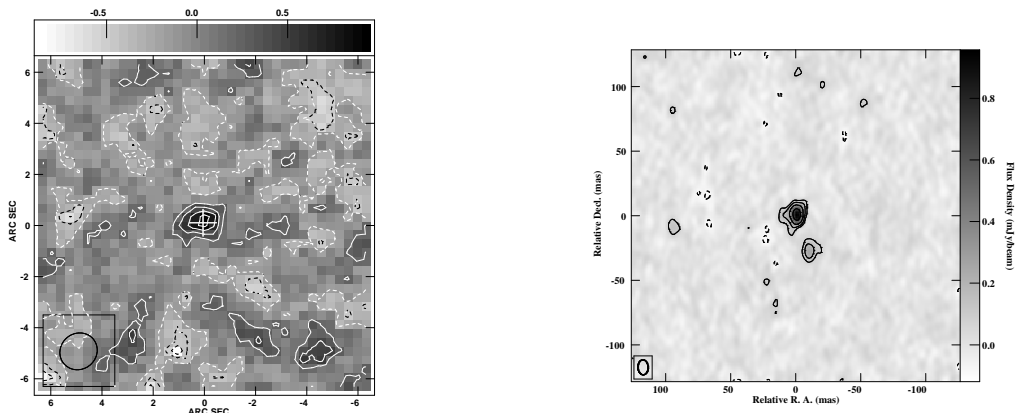


Figure 12: Left: A median stacked image at 1.4 GHz of 6500 Lyman Break galaxies from the COSMOS field ($z \sim 3$, U drop-outs; Carilli et al. in prep). The contour levels are: $-0.75, -0.5, -0.25, 0.25, 0.5, 0.75 \mu\text{Jy beam}^{-1}$. Right: A VLBA image at 1.4 GHz resolution of the most distant radio loud AGN, J1427+3312 at $z = 6.12$. The contour levels are: $-3, 3, 6, 9, 12$ times the rms noise of $28 \mu\text{Jy beam}^{-1}$ (Momjian et al. in prep).

highly confined by the dense ISM of the host galaxy (Taylor et al 1996; Readhead et al. 1996). The conversion efficiency of jet kinetic energy to radio luminosity is thought to increase in such highly confined sources.

While it is dangerous to draw general conclusions from a single source, we can speculate that at the highest redshifts a higher fraction of radio jets will be CSOs, due to the higher gas densities in the earliest galaxies. Kinetic feedback from such jets can affect significantly the evolution of the host galaxy, perhaps inducing star formation, and eventually driving enriched material into the IGM. These radio source also present an ideal opportunity for observations of HI 21cm absorption during cosmic reionization (Carilli et al. 2002).

I should also point out that VLBA observations at 1.4 GHz are reaching (rest frame) brightness temperature sensitivities at mas resolution approaching 10^5 K (Momjian et al. 2007). This limit is critical, since it is the dividing point between the brightness temperature expected for an AGN versus that predicted for a starburst (Condon et al. 1991).

4.5 Complementarity and sensitivity

There are a few important factors to keep in mind when considering SKA phase I studies of high z molecular line emission, in comparison to other, nearer term, telescopes:

- When considering the very first galaxies, into the EoR ($z > 6$), mm telescopes such as ALMA will be limited to studying very high order transitions, eg. at $z = 6$ the lowest ALMA band (80 – 100 GHz) redshifts to 690 GHz, corresponding to CO 6-5, or HCN 7-6. It is unclear that these higher order transitions will be excited in an average galaxy, in particular for the high dipole moment molecules such as HCN, since the required densities for excitation become extreme ($>> 10^5 \text{ cm}^{-3}$).² For comparison, in normal galaxies, such as the Milky

²The CMB will also contribute to excitation. For example, at $z=6$, $T(\text{CMB}) = 19\text{K}$, while the typical CO excitation temperature in an active star forming galaxy is ~ 30 to 40K .

Way, constant T_B holds for the integrated CO emission roughly up to CO 3-2, above which the lines are sub-thermally excited.

- The SKA phase I design corresponds to a collecting area roughly an order of magnitude larger than the EVLA. While the EVLA continuum sensitivity at higher frequencies is a factor 9 improvement over the existing VLA due to the increased bandwidth, the EVLA will have the same collecting area as the VLA, and hence will have at best marginally improved sensitivity for spectral line (ie. band-limited) studies, perhaps 50% due to small improvements in receivers and antenna optics. What the EVLA does provide for line science is improved search capabilities, in terms of new receiver bands and much wider bandwidths with many more channels.
- It should be emphasized that the natural high frequency limit for cm telescopes is ~ 45 GHz, as set by the atmospheric O_2 line. If the SKA phase I was extended to this natural limit, the effective sensitivity is increased by another factor four for thermal objects (assuming constant brightness temperature) relative to a 22 GHz design, improving the SKA phase I to a 40% SKA. A higher frequency would also decrease the necessary longest baseline by a factor two at fixed resolution, thereby reducing the costs of array configuration, connectivity, and data transmission.
- Beyond pointed observations of known high- z objects, the much wider field of view and fractional bandwidth of the SKA relative to eg. ALMA, will allow for efficient surveys for molecular emission line galaxies from $z \sim 2$ into the reionization (Carilli & Blain 2003).

The key point is that, for the first galaxies, the fine structure lines, such as [CII] $158\mu\text{m}$ will be the work-horse lines for ALMA, while studies of molecular gas, the fundamental fuel for star formation in galaxies, will be the regime of short cm wavelength telescopes.

Figure 13 shows the sensitivity to molecular line emission for the EVLA, the SKA phase I, and ALMA. Also shown is a model for the expected continuum and CO line emission from an active star forming galaxy with a total IR luminosity $\sim 10\%$ that of Arp 220 at $z = 5$, corresponding to a star formation rate of a few $10^3 M_\odot \text{ year}^{-1}$. Such a galaxy would be comparable to the Ly α galaxies seen in deep optical surveys at $z \sim 6$, ie. characteristic of the high z galaxy population (Murayama et al. 2007). I have assumed a CO excitation ladder similar to that seen in the few high z molecular line emitting galaxies currently known (this may be biased to higher excitation).

Figure 1 shows that the SKA phase I will be able to detect the CO 1-0 and 2-1 emission from 'normal' star forming galaxies out to very high redshifts, into the epoch of cosmic reionization. ALMA will easily detect the higher order transitions, in sources where they are excited. ALMA will also be able to study the low excitation fine structure line emission from primeval galaxies ([CII] $158\mu\text{m}$, [OI] $63\mu\text{m}$).

For completeness, in Figure 14, I show the continuum sensitivities of these telescopes. The high frequency SKA phase I will easily detect the continuum emission over the rest frame frequency range of 50 to 200 GHz range. The lower end of this range is where free-free emission will dominate, providing the most direct, dust-unbiased, measure of the star formation rate. And the upper end corresponds to the cold dust emission.

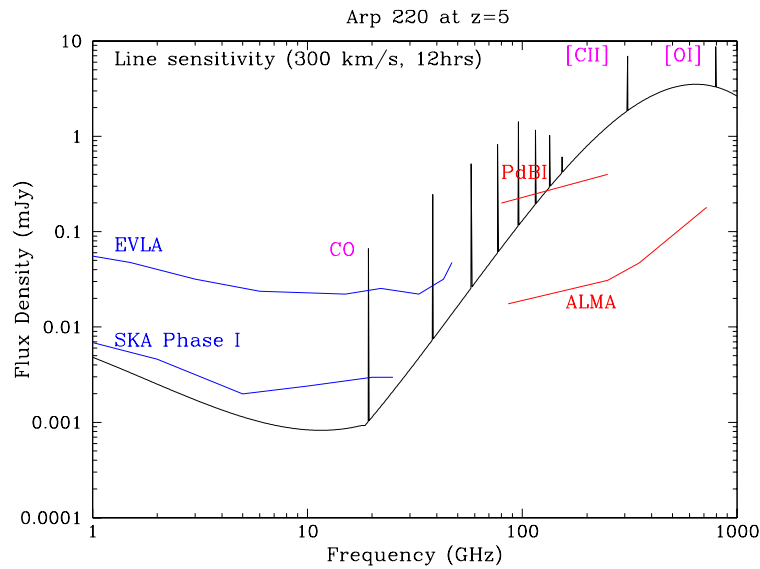


Figure 13: The dotted curves show the (1σ) sensitivity to spectral line emission for the VLA, SKA phase I, and ALMA in 12 hours. The solid curve is the emission spectrum, including continuum and CO lines, for a source with the luminosity of Arp 220 (ie. a source with FIR $\sim 10^{12} L_{\odot}$) at $z = 5$.

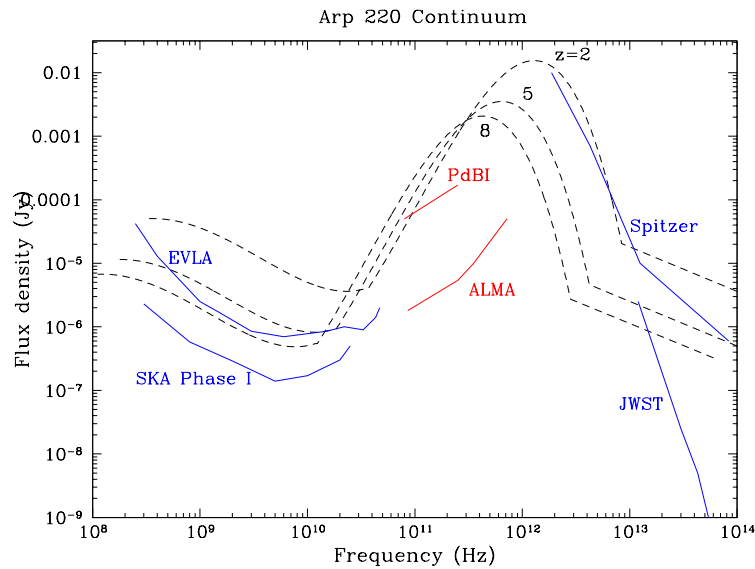


Figure 14: The solid curves show the (1σ) sensitivity to continuum emission for the EVLA, SKA phase I, ALMA, Spitzer, and the JWST, in 12 hours. The dashed curves are the continuum emission spectrum for a source with the luminosity of Arp 220 (ie. a source with FIR $\sim 10^{12} L_{\odot}$) at $z = 2, 5$, and 8 .

Overall, the EVLA Phase III and ALMA provide the necessary complement to large ground and space-based optical and IR telescopes, enabling a panchromatic study of the formation of normal galaxies back to the EoR.

Acknowledgments

CC thanks the Max-Planck-Gesellschaft and the Humboldt-Stiftung for support through the Max-Planck-Forschungspreis. The National Radio Astronomy Observatory is a facility of the National Science Foundation, operated by Associated Universities, Inc.. Thanks also to N. Gnedin, M. McQuinn, M. Zaldariagga, S. Wyithe, W. Lane, W. Cotton, A. Chippendale, E. Momjian, F. Walter for permission to reproduce figures.

References

- [1] Alexander, J. K., Kaiser, M. L., Novaco, J. C., Grena, F. R., Weber, R. R. 1975, *A&A*, 40, p. 365
- [2] Ali, Sk. et al. 2005, *MNRAS*, 363, 251
- [3] Barkana, R. & Loeb, A. 2006, *ApJ*, 624, L65
- [4] Barkana, R., & Loeb, A. 2004, *ApJ*, 601, 64-69
- [5] Barkana, R., Loeb, A. 2005, *ApJ*, 626, 1-11
- [6] Barkana, R. & Loeb, A. 2001, *PhysRep*, 349, 125
- [7] Bertoldi, F., Carilli, C. et al. 2003, *A&A*, 406, L55
- [8] Bertoldi, F., Cox, P., Neri, R. et al. 2004, *A&A*, 409, L47-50
- [9] Bharadwaj, S. & Ali, Sk. 2005, *MNRAS*, 356, 1519-1428
- [10] Burns, J.& Asbell, J., 1991 in *Radio astronomy from space*, NRAO:Greenbank, ed. K. Weiler, p. 29
- [11] Burke, B.F. 1985, in *Lunar bases and space activity of the 21st century*, LPI: Houston, ed. W. Mendell, p. 281
- [12] Bowman, J., Rogers, A., Hewitt, J. 2007, *ApJ*, in press (astro-ph-0710.2541)
- [13] Carilli, C., Hewitt, J., Loeb, A. 2007, "Astrophysics enabled by the return to the moon," ed. M. Livio, (Cambridge University Press) (astro-ph/0702070)
- [14] Carilli, C. et al. 2007, *ApJ*, 666, L9
- [15] Carilli, C. 2006, SKA scientific memo 70
- [16] Carilli, C. et al. 2004, *AJ*, 128, 997
- [17] Carilli, C. et al. 2002, *ApJ*, 577, 22
- [18] Carilli, C. & Blain, A. 2002, *ApJ*, 569, 605
- [19] Carilli, C. 2006, *New Astr.Rev.*, 50, 162
- [20] Carilli, C., Furlanetto, S., Briggs, F., Jarvis, M., Rawlings, S., Falcke, H. 2004, *NewAR*, 48, 1029-1038
- [21] Cen, R. 2003a, *ApJ*, 591, 12-37

- [22] Cen, R. 2006, ApJL, submitted (astro-ph/0601010)
- [23] Chen, X. & Miralda-Escude, J. 2004, ApJ, 602, 1-11
- [24] Ciardi, B., & Ferrara, A. 2005, Space Science Reviews, 116: 625-705
- [25] Ciardi, B., Madau, P. 2003, ApJ, 596, 1-8
- [26] Condon, J.J. et al. 1991, ApJ, 378, 65
- [27] Cotton, W., Condon, J., Perley, R. et al. 2004, SPIE, 5489, 180-189
- [28] Cowie et al. 1996, AJ, 112, 839
- [29] Dennison B., Turner B. E., Minter A. H., 2005, ApJ, 633, 309
- [30] Di Matteo, T., Rosalba, P., Abel, T., Rees, M. 2002, MNRAS, 564, 576-580
- [31] Di Matteo, T., Ciardi, B., & Miniati, F. 2004, MNRAS, 355, 1053 - 1065
- [32] Ellingson, S. 2005, Exp. Astron., 17, 261-267
- [33] Ellis, R. 2006, Saas Fe Advanced Course 36 Swiss Soc. Astrophys. Astron. in press.
- [34] Ershov A. A., 1987, Soviet Astronomy Letters, 13, 115
- [35] Falcke, H. 2006, *IAU JD12: Long Wavelength Astrophysics*, 12, 16
- [36] Fan, X. et al. 2006, AJ, 132, 117
- [37] Fan, X., Carilli, C., Keating, B. 2006, ARAA, 44, 415
- [38] Fan, X., et al. 2004, AJ, 128: 515-522
- [39] Furlanetto, S., & Loeb, A. 2002, ApJ, 579, 1-9
- [40] Furlanetto, S., Zaldarriaga, M. Hernquist, L. 2004, ApJ, 613, 16-22
- [41] Furlanetto, S. et al. 2006, Physics Repts, 433, 181
- [42] Furlanetto, S., Sokasian, A., Hernquist, L. 2004, MNRAS 347, 187-195
- [43] Furlanetto, S., McQuinn, D., Hernquist, L. 2005, MNRAS, 365, 115
- [44] Furlanetto, S. 2006, MNRAS, 370, 1867
- [45] Gleser, L. et al. 2007, ApJ, in press (astro-ph/0712.0797)
- [46] Gnedin, N. 2004, ApJ, 610, 9-13
- [47] Gnedin, N. & Shaver, P. 2004, ApJ, 608, 611-621
- [48] Gorgolewski, S. 1965, Astronautica Acta, New Series 11, 126, 130
- [49] Haverkorn, M., Katgert, P., de Bruyn, A. 2004, A& A, 427, 549-559
- [50] Heckman, T. et al. 2004, ApJ, 613, 109
- [51] Iliev et al. 2006, MNRAS, 369, 1625
- [52] Kuiper, T., Jones, D., Mahoney, M., Preston, R. 1990, in *Astrophysics from the moon*, New York: AIP, p. 522
- [53] Lane, W., Cohen, A., Cotton, W., et al. 2004, SPIE, 5489, 354-361
- [54] Lazio, J. et al. 2006, *IAU JD12: Long Wavelength Astrophysics*, 12, 62

- [55] Li, Y., Herquist, L., Robertson, B. et al. 2007, *ApJ*, 665, 187
- [56] Lidz, A. et al. 2007, *ApJ*, in press (astro-ph/0711.4373)
- [57] Livio, M. 2006, "Astrophysics enabled by the return to the moon: conference summary," ed. M. Livio, (Cambridge University Press)
- [58] Loeb, A., Barkana, R. 2001, *ARAA*, 39, 19-66
- [59] Loeb, A. & Zaldarriaga, M. 2004, *Phys.Rev. Lett.* 92, 1301-1304
- [60] McGreer, I. et al. *ApJ*, 652, 157
- [61] Mcquinn, M. et al. 2006, *ApJ*, 653, 815
- [62] Momjian, E. et al. 2007, *AJ*, 134, 694
- [63] Morales, M. & Hewitt, J. 2004, *ApJ*, 615, 7-18
- [64] Morales, M. 2005, *ApJ*, 619, 678-683
- [65] Murayama, T. et al. 2007, *ApJS*, 172, 523
- [66] Narayanan, D. et al. 2007, *ApJ*, in press (astro-ph/0711.1361)
- [67] Oh, S.P. & Mack, K. 2003, *MNRAS*, 346, 871-877
- [68] Omont, A. et al. 2003, *A&A*, 398, 857
- [69] Readhead, A. et al. 1996, *ApJ*, 460, 612
- [70] Riechers, D. et al. 2007, *ApJ*, 671, L13
- [71] Santos, M., Cooray, A., Knox, L. 2005, *ApJ*, 625, 575-587
- [72] Sethi S. K., Subrahmanyan R., Roshi D. A., 2007, *ApJ*, 664, 1
- [73] Sethi, S. 2005, *MNRAS*, 363, 818
- [74] Shapiro, P. et al. 2006, *ApJ*, 646, 681
- [75] Taylor, G. et al. 1996, *ApJ*, 463, 95
- [76] Walter, F., Bertoldi, F., Carilli, C., et al. 2003, *Nature*, 424, 406-408
- [77] Walter, F., Carilli, C., Bertoldi, F. et al. 2004, *ApJ*, 615, L17-20
- [78] Wang, R., Carilli, C. et al. 2007, *AJ*, 134, 617
- [79] Waon, G. et al. 1997, *ESA Sci(97)* 2
- [80] Wyithe, J.S., Loeb, A., Barnes, D. 2005, *ApJ*, 634, 715
- [81] Wyithe, J.S., Loeb, A., Carilli, C. 2005, *ApJ*, 628, 575-582
- [82] Zahn, O. et al. *ApJ*, 654, 12
- [83] Zaldarigga, M., Furlanetto, S., Henquist, L. 2004, *ApJ*, 608, 622-635